

H_∞ CONTROL DESIGN OF FLEXIBLE ROTOR MAGNETIC BEARING SYSTEM

F. Carrère

Société de Mécanique Magnétique
27950 Saint-Marcel, France

S. Font, G. Duc

École Supérieure d'Électricité
91192 Gif-sur-Yvette Cedex, France

ABSTRACT

A method to design robust controller for flexible rotor magnetic bearing system is considered using H_∞ multi-blocks standard problem optimization. We described how to take into account controller specifications such as disturbance rejection in bandwidth, modes damping, roll-off behaviour, model uncertainties, by elaborating an augmented plant model with supplementary degrees of freedom on the input and output of the flexible modes.

A mathematical model of flexible rotor with six bending modes is taken as reference model and this approach allows to get a same order controller that we can reduce by an appropriate method. Continuous and digital syntheses are shown.

This way should allow to conveniently tune closed loop behaviour while satisfying severe constraints on the control capability and should result in a practical realization for controller implementation.

INTRODUCTION

H_∞ approaches appear to be a powerful and extremely versatile tool to determine the achievable performance in AMB systems and to design the corresponding controllers. To be used in industrial applications, we need to take into account number of engineering specifications and constraints not limited to single specification regarding disturbance attenuation with simple reference model. In the same way, we examine in this paper the design of flexible rotor system with AMB control because they are concerning most of non repetitive and particular machines in the heavy industry with generally very well defined customer specifications. This method could be a methodical way to design robust controllers if objectives, that we defined in this paper, are well done. So, we want to focus on specifications regarding performance stiffness, damping on bending modes, robustness regarding to model uncertainties or

gyroscopic effects which could be reduced in this case as multiplicative errors and robustness on higher frequencies (it's not true for very high gyroscopic effects).

Classical criteria using H_∞ method are generally unable to satisfy closed loop behaviour for flexible rotor because it is difficult to satisfy both stiffness performance, control effort and robustness on higher modes: in very often case, supercritical rotor has a very high damping constraint on first bending mode (as $\zeta \geq 15\%$) and spill-over problem could be difficult to solve. So, we propose an alternative to the "mixed sensitivity problem" by a generalization of a four blocks problem [1].

In addition to these objectives, a lot of papers concerning synthesis of robust controllers for flexible structure using H_∞ method achieve high order controllers limiting this approach to a school case. So, some industrial researches deal with practical methods to get "a priori" low order controllers [2]. This approach, showed in this paper, can be viewed as a generalization of some of these methods to take into account particular case of an AMB system.

DESIGN OBJECTIVES AND MULTI-BLOCK H_∞ DESIGN

H_∞ optimization takes now an important place in the control literature [3,4,5]. It is concerned with the optimization of different transfer functions of a closed loop system. Consider for instance the block-diagram of **FIGURE 1**, where $K(s)$ is the controller to be designed and $G(s)$ a model of the plant ; b and d being disturbances acting at the input and the output of the plant respectively, u is the variable received by the plant, and y the output to be regulated. Denote $T_{z/w}$ the transfer function from an input w to an output z of the closed loop system.

The most usual H_∞ optimization problems are the following ones :

$$\left\| \begin{bmatrix} w_1 T_{y/d} w_d \\ w_2 T_{u/d} w_d \end{bmatrix} \right\|_\infty < 1 \text{ (mixed sensitivity problem) (1)}$$

where W_1, W_2 are frequency dependent weighting functions : in general they are chosen to penalize $T_{y/d}$ at low frequencies and $T_{u/d}$ at high frequencies. W_d can be viewed as a generator of the disturbance d .

Considering FIGURE 1 feedback considerations, we get an optimization problem as:

$$\left\| \begin{bmatrix} w_1 T_{y/d} w_d & w_1 T_{y/b} w_u \\ w_2 T_{u/d} w_d & w_2 T_{u/b} w_u \end{bmatrix} \right\|_\infty < 1 \text{ (four block problem) (2)}$$

This latter form is known to give more balanced input and output performances, since it takes into account input and output disturbances [10]. It also avoids pole/zero cancellations between the controller and the plant model, which would be undesirable in the case of lightly damped plant poles [8].

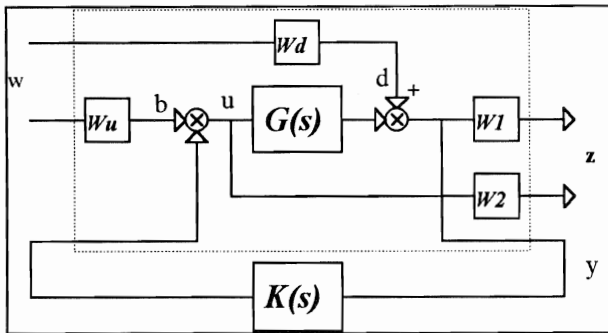


FIGURE 1 : Feedback configuration

In this study, regulation problem can be reduced to a multi SISO problem and process model is given in a state space as a rigid mode with $n=6$ flexible modes, whose damping ratio is assumed to be very small ($10^{-3} < \zeta < 10^{-2}$).

Considering the state vector with modal coordinates $\{q_1, \dot{q}_1, \dots, q_{2n_r+2}, \dot{q}_{2n_r+2}\}$, we can establish a state space model of a free-free rotor in a modal form:

$$\begin{cases} \dot{X} = AX + BU \\ Y = CX \end{cases}, \text{ with } \begin{matrix} X = \text{measurement vector} \\ U = \text{force command vector} \end{matrix}$$

A is a diagonal matrix :

$$A = \begin{pmatrix} 0 & 1 & & & & \\ -\omega_0^2 & -\lambda_0 & & & & \\ & & \ddots & & & \\ & & & 0 & 1 & \\ & & & & & -\omega_v^2 & -\lambda_v \end{pmatrix}, B = \begin{pmatrix} 0 \\ \phi_0 \\ \vdots \\ 0 \\ \phi_v \end{pmatrix}, X = \{\phi_1^t \ 0 \ \dots \ \phi_v^t \ 0\}$$

State space model (3)

Matrix B and C are eigenvectors for respectively bearing nodes and detection nodes with $\lambda_i = 2\zeta\omega_i$ for a damped structure. The first diagonal block with $\omega_0 \neq 0$ is relative to the rigid mode.

In practical applications, the control design should be applied to the full order system due to interaction between a low order command model and residual system. The full order system may be destabilized or has a very poor robustness on high frequency range. So, this method is based on a command model taken as a transfer function with $n=6$ (mode number) issue from (3). General form is:

$$G(s) = \sum_{i=0}^n \left[\frac{\alpha_i}{s - p_i} + \frac{\alpha_i^*}{s - p_i^*} \right] \quad (4)$$

The closed loop objective is first to insure a bandwidth between $2\pi \times 50$ rd/s and $2\pi \times 60$ rd/s to assume the required stiffness as specified. This value corresponds to the one required for the "rigid body" modes. The corresponding damping ratio has to be greater than 0.5 to limit the resonance of the frequency response, and thus the deviation of the rotor, when the rotation speed is equal to this frequency.

These performances characteristics are well known to define the W_1 weighting function which can be expressed as constraints on an ideal shape of the controller, with integral action inside the bandwidth and a limited gain in the modal region defining the quality factor (no greater than 3dB).

The working rotation speed being beyond the first bending mode (the machine is said to be "supercritical"), this mode has also to be damped. It is, however, important to note that the electronic amplifiers introduce a severe limitation to the control capability ; it is therefore not easy to obtain a damping ratio greater than 0.2 for the first bending mode, while the other modes can also be damped, but with decreasing damping ratios.

These specifications defined the second objective in term of expected roll-off as -20dB/decade up to the second bending mode; W_2 weighting function will be chosen to take into account this specification, as well as saturation condition on control effort.

Nevertheless, standard criteria such as (2) are not completely satisfactory to insure a good closed loop behaviour because only inputs and outputs of the plant, as described by $G(s)$, are considered in such problems. In order to obtain supplementary degrees of freedom, the input and the output of the flexible modes are also introduced in the criterion, with constant scaling.

Continuous-time synthesis

The H_∞ optimization problem has been formulated according to the block diagram of FIGURE 2 : the plant model is separated into 7 transfer functions

(see eq.4) corresponding to the rigid mode (*inert*) and the 6 bending modes (*mod1* to *mod6*). Supplementary inputs $e_1 \dots e_6$ and outputs $s_1 \dots s_6$ have been added : the input e_i is exciting the i -th mode only in order to force the controller to take into account the corresponding frequency explicitly. Similarly the output s_i of the i -th mode is used to underline that the corresponding frequency has to remain non excited and to control the resonance of the mode. This approach can be viewed as a generalization of the one proposed in [2], where only the disturbance d and the outputs of the modes were appearing.

According to this block diagram, the H_∞ optimization problem is written as follows:

$$\gamma = \left\| W_{out} T_z / W_{in} \right\| < 1 \quad (5.1)$$

where

$$z = [y \ u \ s_1 \ s_2 \ s_3 \ s_4 \ s_5 \ s_6]^t \quad (5.2)$$

$$w = [d \ b \ e_1 \ e_2 \ e_3 \ e_4 \ e_5 \ e_6]^t \quad (5.3)$$

$$W_{out} = \text{diag} \{ W_1(s), W_2(s), W_{s_1}, W_{s_2}, W_{s_3}, W_{s_4}, W_{s_5}, W_{s_6} \} \quad (5.4)$$

$$W_{in} = \text{diag} \{ W_b, W_{e_1}, W_{e_2}, W_{e_3}, W_{e_4}, W_{e_5}, W_{e_6} \} \quad (5.5)$$

and all weighting functions are constant scalars, except $W_1(s)$ and $W_2(s)$ which are frequency dependent.

Now, the minimization problem is augmented with

criteria such as $\| w_{si} \text{ mod}_i (I + GK)^{-1} w_{ei} \|_\infty < 1$, where w_{si} acts to avoid pole/zero cancellations (since w_{si} penalizes $G_i(I+GK)^{-1}$). Weighting these terms allow to adjust independently the damping factors. w_{ei} adds uncertainties to take into account model uncertainties or variations (as low gyroscopic effects).

Such weighting functions allow to trade the different objectives; since they are constant, the order of the augmented plant for the H_∞ problem is not increased. Their selection is discussed in the next subsection.

Selection of the weighting functions

As explained in previous chapter, the choice of the two frequency-dependent functions $W_1(s)$ and $W_2(s)$ is standard [7]: $W_1(s)$ is a low-pass filter in order to choose the bandwidth of the closed loop and to reduce the output deviation at low frequencies by introducing a quasi-integral action in the controller ; $W_2(s)$ is a high pass filter in order to reduce the control effort at high frequencies by introducing an appropriate roll-off in the controller. Selected filters are the following ones:

$$W_1(s) = 10^4 \frac{\frac{s}{3} + 2\pi \times 70}{s + 2\pi \times 70} \quad (6.1)$$

$$W_2(s) = \frac{1}{40} \frac{s + 2\pi \times 100}{\frac{s}{20} + 2\pi \times 100} \quad (6.2)$$

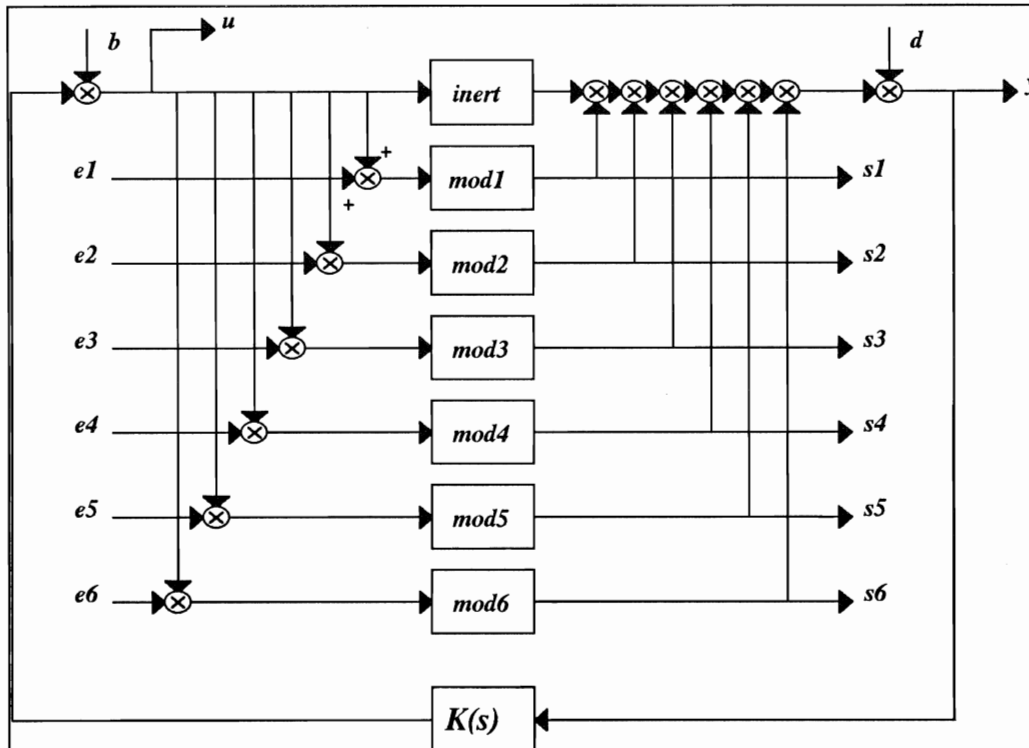


FIGURE 2: Block diagram of the H_∞ synthesis

As soon as setting these function parameters, it is possible to start an iterative process to find appropriate constant factors according to specified constraints. The constant scalar W_b is then selected. To this end the problem (5) is solved with $W_{e_i} = 0, W_{s_i} = 0$ (which yields a four block problem).

For small values of W_b (i.e. $W_b \approx 10^{-3}$) we obtain $\gamma \ll 1$ because $W_1(s)$ and $W_2(s)$ have been chosen to give a little constrained problem, and the transfer functions $T_{y/b}$ and $T_{u/b}$ are unconstrained. By gradually increasing the value of W_b , one of these functions becomes constrained and the value of γ increases.

The same procedure is used to introduce gradually the weighting scalars W_{e_i}, W_{s_i} . The weighting factors which correspond to the most higher mode are introduced first, i.e. we consider successively: $W_{s_6}, W_{e_6}, W_{s_5}, W_{e_5}, \dots, W_{s_1}, W_{e_1}$.

With this problem the controller order is the same as the command model augmented with an integral term and a low pass filter; this compensator will further be reduced to realistic controller.

RESULTS

FIGURE 3 shows the 4 main transfers of the closed loop system which appear in the criterion, compared with their constraints defined by the weighting

functions (the regions of high constraint are underlined).

It is clear that $W_1(s)$ constraints $T_{y/b}$ at low frequencies and $T_{y/d}$ around the bandwidth, insuring a good disturbance attenuation and small enough resonances ; $W_2(s)$ constraints $T_{u/d}$ in the modal region, which is important to limit the control effort.

FIGURE 4 illustrates the effect of the modes and outputs introduced in the criterion : an increased damping ratio is clearly obtained for the first two modes while no significant effect is obtained for the last ones, due to the limitation of the control variable at high frequencies.

TABLE 1 shows the damping ratios obtained at the crossover frequency and for the first 3 bending modes. The Bode diagram of the controller is given on FIGURE 6. These results are in accordance with the objectives given above.

Finally the Nichols chart of the controlled plant is given on FIGURE 5 (the dashed curves correspond to closed loop resonances of 1dB, 3dB, 6dB respectively). This plot underlines the main features of the control problem : the integral action combined with the inertia yields an argument of -270° up to the neighbourhood of the crossover frequency, while the first bending mode appears just beyond it. One can also

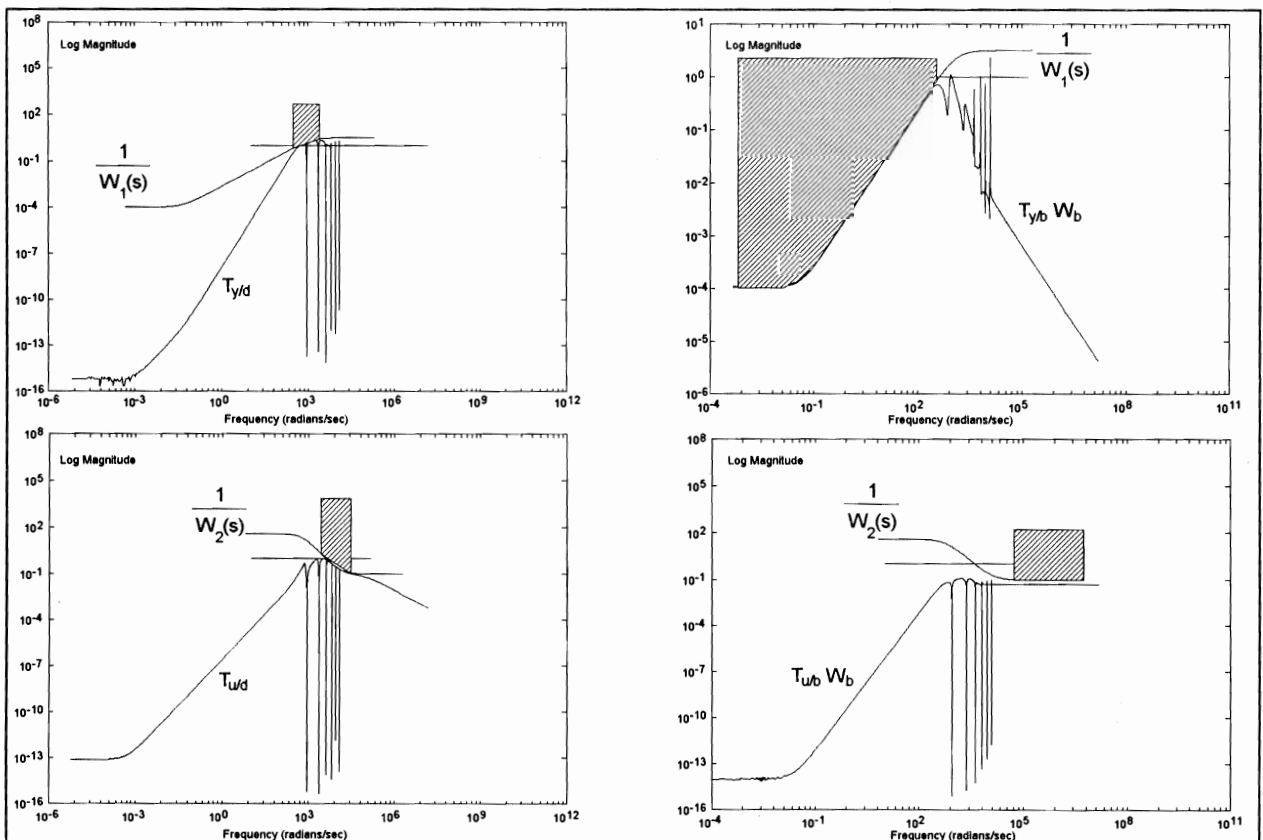


FIGURE 3: Main transfers of the closed loop system

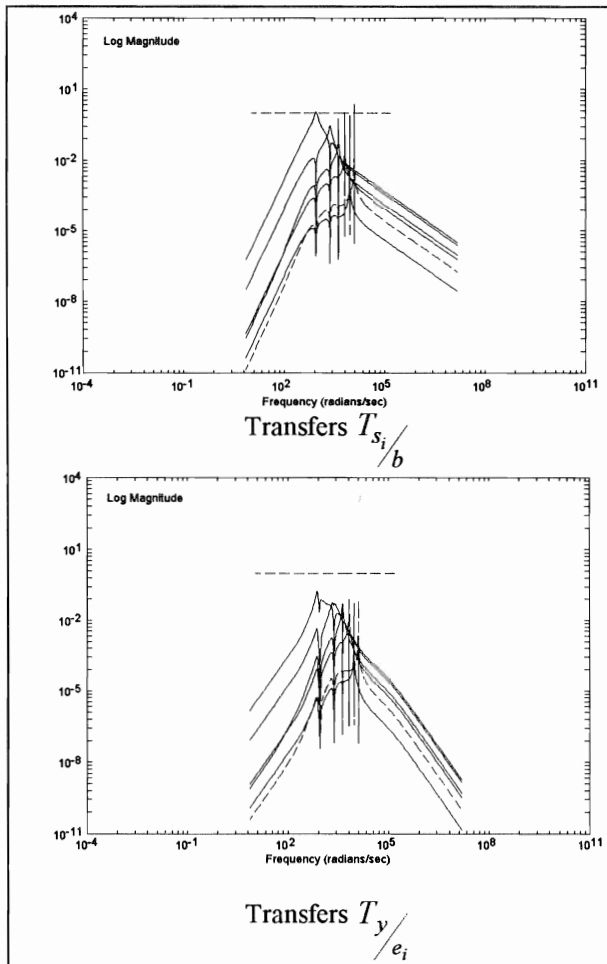


FIGURE 4 : Some transfers related to inputs/outputs of the modes

see that the controller places the other modes between the critical points ($0dB, (2k+1)180^\circ$) - the centre of the dashed curves - and that the 5th and 6th modes are rejected below the $0dB$ line.

4. REDUCED ORDER CONTROLLER

Although the proposed criterion yields a controller

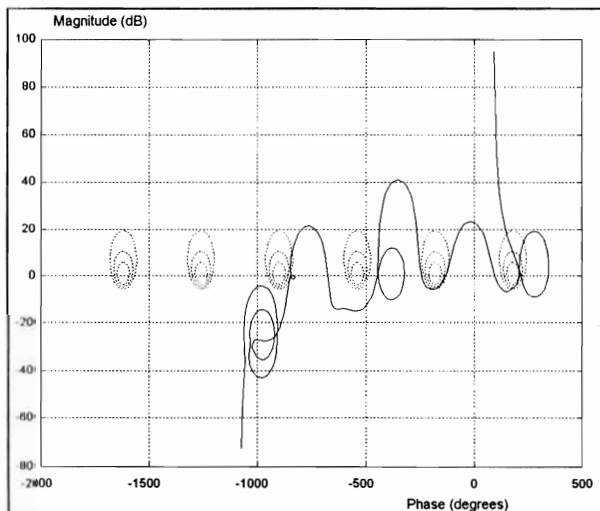


FIGURE 5 : Nichols charts of the controlled plant

of reasonable order (order 17 in this case), its implementation will become more easier when using a reduction procedure. Instead of applying the popular balanced truncation technique [6] we used the aggregation method developed in the 70's [9] : as an advantage, it allows to choose the most important poles of the controller, which will be exactly retained in the reduced order one.

FIGURE 6 shows the Bode diagrams of controllers of order 13 and 10, compared with the controller previously designed : the response of the controller is well preserved up to the modal region, while the only differences appear for the 10th order controller at high frequencies.

FIGURE 7 shows the Nichols chart of the controlled plant with the 10-th order controllers : it clearly shows that the control strategy has not been affected by the

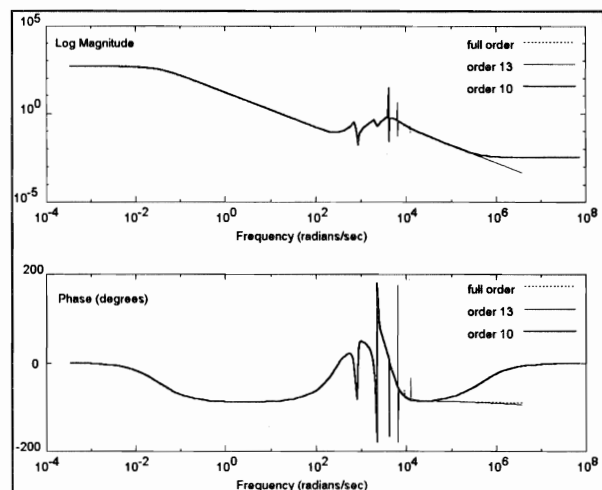


FIGURE 6: Bode plot of the continuous-time controllers

reduction procedure. As indicated on Table 1, the same damping ratios are obtained as for the full order controller.

5. DISCRETE-TIME SYNTHESIS

To obtain a digital controller, a procedure similar to the one developed in the previous sections can be applied :

a) determine $G_d(z)$ the discrete-time transfer function of the plant with sampling period T_e and zero-order hold.

b) apply the bilinear transform $s \rightarrow \frac{2/T_e + s}{2/T_e - s}$ to

define an equivalent continuous-time transfer function transfer $G_{eq}(z)$.

c) design a continuous-time H_∞ controller $K(s)$ for $G_{eq}(z)$

d) obtain the digital controller $K_d(z)$ by applying the reverse transform $s \rightarrow \frac{2}{T_e} \frac{z-1}{z+1}$ to $K(s)$.

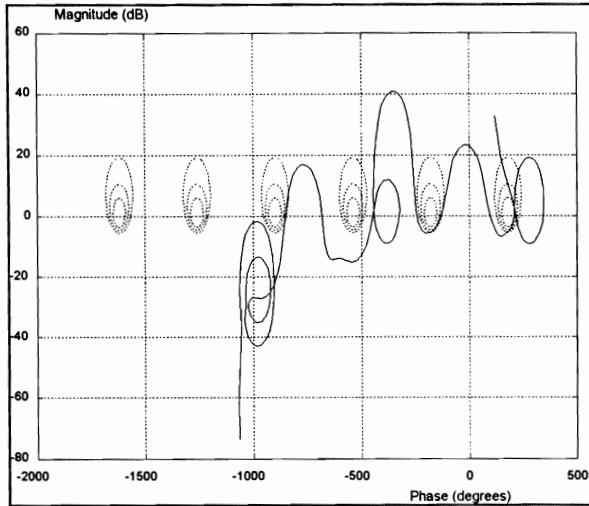


FIGURE 7 : Nichols chart, with 10th order controller

| | Continuous | Continuous (reduced) | Discrete (reduced) |
|-------------|------------|----------------------|--------------------|
| Cross-over | 0.66 | 0.66 | 0.66 |
| 1st mode | 0.104 | 0.105 | 0.140 |
| 2nd mode | 0.070 | 0.076 | 0.061 |
| 3rd mode | 0.028 | 0.027 | 0.015 |
| other modes | < 0.01 | < 0.01 | < 0.01 |

TABLE 1 : Damping ratios of the main closed-loop poles.

It is well known that the bilinear transform used at steps b) and d) maps the imaginary axis $Re(s) = 0$ onto the unit circle $|z| = 1$, preserving the closed loop stability and the H_∞ -norm : γ being the value of the criterion (5) obtained at step c), the same value is therefore obtained when applying $K_d(z)$ to $G_d(z)$. Note that if $G_d(z)$ has no pole on the unit circle, this property holds for any value of T_e .

From a practical point of view, it is however more convenient to choose a small enough sampling period T_e : $G(s)$ and $G_{eq}(s)$ have then similar frequency responses, so that the weighting functions $W_1(s)$ and $W_2(s)$ chosen for $G(s)$ remain convenient for $G_{eq}(s)$: A sampling period of 0.2ms has been chosen : it is high enough to allow the implementation of a controller of order less than 14, and the sampling rate is greater than twice the higher frequency of the modes.

FIGURE 8 shows the Bode diagram of the equivalent continuous-time controller $K(s)$, which has

been reduced to order 13. FIGURE 9 gives the Nichols chart of both controlled systems $K(s)G_{eq}(s)$ and $K_d(z)G_d(z)$. These plots clearly establish that the control strategy obtained for the continuous-time synthesis is well duplicated. In fact Table 1 indicates that similar damping ratios are obtained for the cross-over frequency as well as for the bending modes.

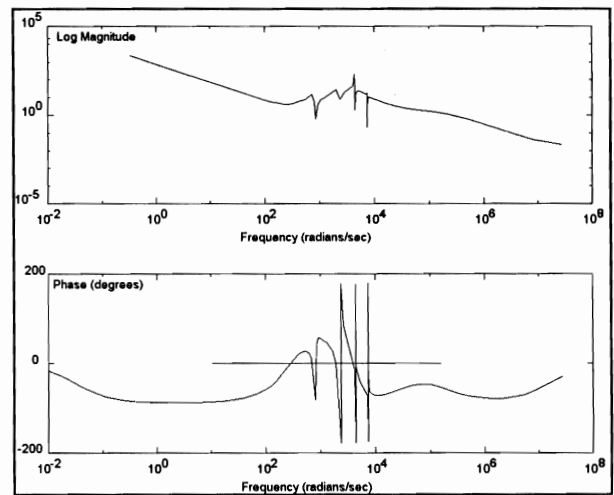


FIGURE 8 : Bode diagram of the 13th order equivalent continuous-time controller

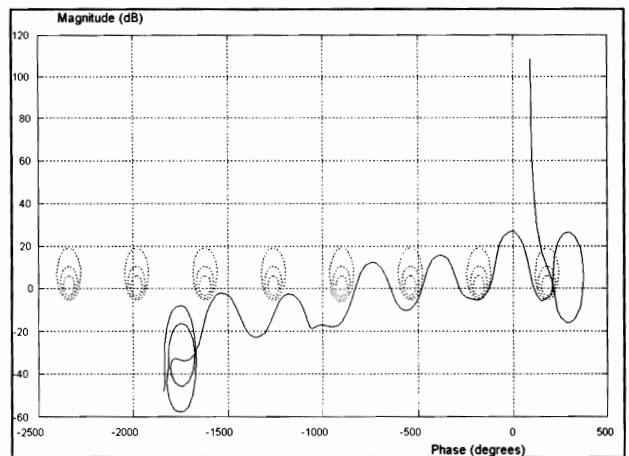


FIGURE 9 : Nichols chart of the discrete-time controlled plant

6. CONCLUSION

The control of a magnetic bearing has been considered in this paper, using H_∞ multi-block optimization, to give versatile and methodical criteria corresponding to known specifications in most of industrial applications. The process being characterized by a number of lightly damped bending modes was generating realistic controllers, since its order is not higher than a command model. So the discrete-time synthesis proves that it is relatively easy to implement a 13th order controller on a DSP with high sample frequency.

This study allows to remove limits farther in the H_∞ design, since we have increased supplementary degrees of freedom without increasing problem complexity. A complete study with a multivariable design and an adequate robustness analysis should yield to a fully operational way in applications.

7. REFERENCES

- [1] S. Le Ballois, G.Duc, " H_∞ control of a satellite platform, coprime factor design versus multi-blocks approach", Vancouver (Canada), sept 93, 2nd IEEE conf. on control applications.
- [2] P. Coustal, J. M. Michelin, "Iterative synthesis of low order controller for flexible structure using H_∞ methods," *Proc. Europ. Contr. Conf. ECC 93*, pp. 727-732, Groningen, The Netherlands, June 1993.
- [3] J. Doyle, K. Glover, P. Khargonekar, B. Francis, "State-space solutions to standard H_2 and H_∞ control problems," *IEEE Trans. Auto. Contr.*, Vol. 34, pp. 831-846, August 1989.
- [4] H. Kwakernaak, "Robust Control and H_∞ -Optimization A Tutorial Paper," *Automatica*, Vol. 29, No 2, pp. 255-273, March 1993.
- [5] D. Mc Farlane and K. Glover, "Robust Controller Design Using Normalised Coprime Factor Plant Descriptions," *Lecture Notes in Control and Information Sciences*, Springer Verlag, 1990.
- [6] D. Mustafa, K. Glover, "Controller Reduction by H_∞ -Balanced Truncation," *IEEE Trans. Auto. Contr.*, Vol. 36, pp. 668-682, June 1991.
- [7] I. Postlethwaite, Mi-Ching Tsai, Da-Wei Gu, "Weighting function selection in H_∞ design," *Prepr. 11th IFAC World Congress*, Vol. 5, pp. 104-109, Tallin, Estonia, August 1990.
- [8] J. Sefton, K. Glover, "Pole / zero cancellations in the general H_∞ problem with reference to a two-bloc design," *Syst. Contr. Lett.*, Vol. 14, pp. 295-306, April 1990.
- [9] J. M. Siret, G. Michailesco, P. Bertrand, "On the Use of Aggregation Techniques," in *Handbook of Large Scaled Systems Engineering Applications*, pp. 20-27, M. Singh and A. Titli Edts, North-Holland, 1979.
- [10] S. J. Williams, R. A. Hyde, "A comparison of different H_∞ methods in VSTOL flight control system design," *Proc. Amer. Contr. Conf.*, San Diego, CA, June 1990.

